Assessing fuel consumption reduction in Revercycle, a reversible mobile air conditioning/ Organic Rankine Cycle system

Luca Di Cairano, W. Bou Nader, M. Nemer

ASSESSING FUEL CONSUMPTION REDUCTION IN REVERCYCLE, A REVERSIBLE MOBILE AIR CONDITIONING/ ORGANIC RANKINE CYCLE SYSTEM

L. Di Cairano[1]*, W. Bou Nader[2], M. Nemer[3]

[1]MINES ParisTech, PSL Research University, Center for Energy Efficiency of Systems
Palaiseau, France
luca.di_cairano@mines-paristech.fr

[2]PSA Group, Centre Technique de Vélizy,
Vélizy, France
wissam.bounader@mpsa.com

[3]MINES ParisTech, PSL Research University, Center for Energy Efficiency of Systems
Palaiseau, France
maroun.nemer@mines-paristech.fr

* Corresponding Author

ABSTRACT

Organic Rankine Cycle (ORC) is a promising solution to improve vehicle efficiency, but its commercial success is hindered by the compactness and cost requirements of the automotive sector. In an attempt to overcome these limitations, a reversible mobile air conditioning (MAC)/ORC, hereafter called ReverCycle, is proposed in this work. ReverCycle is a compact system that operates in two different modes: a standard MAC system when cabin cooling is required or an ORC recovering mechanical energy from the waste heat of an engine's cooling system.
This study presents a simulation methodology to assess the ReverCycle fuel consumption gain. A global light duty vehicle model allows the estimation of the yearly working hours for each ReverCycle operating mode and quantifies the recovered mechanical energy in ORC mode. The ORC module is validated with experimental results. Validation has shown a normalized root-mean-square deviation between 5% and 11% for the main ORC variables (pressures, temperatures and electric powers).
The average fuel consumption reduction in ReverCycle was 1.3 and 2% with cold start and hot start conditions, respectively. The reversible system lost 25% of the ORC waste heat recovery potential owing to MAC activation time; however, the significant reductions in cost and compactness were advantageous.

KEYWORDS

Waste heat recovery, reversible scroll machine, Organic Rankine Cycle, mobile air conditioning, conventional vehicle

HIGHLIGHTS

- ReverCycle is a low cost and compact waste heat recovery solution
- A global vehicle model is used to correctly assess the real life fuel economy
- ReverCycle fuel economy ranges from 1.3% at cold start to 2% at hot start in Paris region

1. INTRODUCTION

The transport sector has a strong impact on CO_2 emissions. Therefore, regulatory organizations have been imposing strict limits for fuel consumption and emissions on car manufactures. Many technical solutions are under study to meet these requirements; among them, waste heat recovery has garnered significant attention. In a passenger car, almost 60% of the fuel chemical energy is lost to the environment as waste heat[1,2]. The two available heat sources in a vehicle are the engine coolant and exhaust gases. The first has the advantage of having stable temperature with a mean close to 100 °C, while the second is a higher quality energy source with a highly fluctuating temperature that can reach 900 °C [3].

The most promising technologies identified in literature are Rankine cycle (RC) or Organic Rankine Cycle (ORC) [4,5], thermoelectric generators [6,7], turbocompounding [8] and thermoacoustic converters. Thermoelectric generators (TEG) directly convert engine waste heat into electricity thanks to Seebeck effects .TEG is a silent system without rotating parts, but its thermal efficiency is low and its integration into a vehicle implies radiator oversizing [9] and an important added cost. Turbocompounding consists in adding a power turbine on the exhaust gases. It is a very compact and light system, but its limits are the turbine efficiency and backpressure losses [8]. Thermoacoustic converters are another possible waste heat recovery solution. Waste heat is converted to acoustic energy, that is then converted to mechanical or electric energy. As TEG, thermoacoustic converter is a system without moving parts. Unfortunately, there are many disadvantages. Performance is strongly affected by heat losses and streaming [10]. In addition, this kind of converter presents structural integrity problems and vibrations [11].

The main difference between an RC and ORC is the working fluid. In ORCs, an organic fluid is used instead of water to obtain higher efficiencies with low temperature sources.

The integration of RC and ORC in passenger cars is a difficult task, compared to heavy duty vehicles, because of the compactness requirements and the dynamic working regime [12]. Furthermore, the additional weight introduced by the ORC/RC components and their interaction with other vehicle systems negatively impacts the performance [13]. BMW researchers investigated more interesting methods to simplify the complexity and reduce the weight of their RC system instead of maximizing the power output [14]. Their Turbosteamer is a Rankine cycle embedded prototype recovering waste energy from the exhaust gases of a BMW 5 series. Once optimized it could provide a 4% fuel economy improvement [13].

Most of previous research work on automotive RC/ORC has focused on exhaust gases because of their higher exergy content [15,16] and better performances at cold start [17] compared to WHR from engine coolant. However, some issues are reported like backpressure losses, low available energy at low speed and constraints on expander inlet temperature involving important exergy destruction (e.g. 300°C in [13]).

Recently, engine coolant as a heat source has become increasingly popular [17–19] because it can help in developing a lightweight and low-cost solution [20]. If the system cost is strongly reduced, the payback time could be shorter even with a low fuel economy gain. The pseudo-constant temperature level of the engine coolant is another advantage allowing a better optimization of the ORC components. Smague et al. [20] concluded that a potential of 2% and up to 3% fuel economy improvement is possible in an ORC for waste heat recovery from the coolant of a light duty vehicle. However, it is noteworthy to mention that, while the 4% fuel economy improvement announced by Horst et al. [13] is based on the feedback of the Turbosteamer prototype, the fuel economy improvement announced by Smague et al. [20] is based on an early development phase.

In engine coolant heat recovery, an important cost reduction is achievable by selecting off the shelf components of the automotive air conditioning system [21]. A low-level heat source has the advantage to be compatible with the exploitation of automotive scroll compressors as expanders in the ORC cycle[22,23]. This feature can help in developing a reversible system as that in [24].

In this work, the engine coolant is chosen as waste heat source. This low temperature source simplifies the development of a reversible MAC/ORC system; it allows using in ORC mode the same working fluid as in MAC mode (R134a, R1234yf). In addition, thanks to lower temperature constraints, an automotive scroll compressor can be easily converted into a reversible compressor/expander.

This work presents ReverCycle, a reversible MAC/ORC system, wherein the ORC hot source is the engine coolant to benefit from the important cost reductions.
The primary goal of this study is to assess the fuel economy of this innovative system. The second goal is to estimate the waste recovery potential lost due to the MAC activation time. A reversible system implies that the ORC function is not available when MAC is turned on.

2. SYSTEM OUTLINE AND DESIGN

2.1 Operating Mode

Figure 1 shows the architecture of the system. The refrigerant R134a is selected as the initial working fluid for this study and that for the proof of concept. The final working fluid choice will be its substitute, R1234yf. Two components are mutualized, namely the scroll machine and MAC/ORC condenser. The scroll machine is mechanically coupled with the engine shaft. The machine can operate as a compressor and expander in the MAC and ORC modes, respectively. The operating mode is switched by the activation and deactivation of two automatic valves.

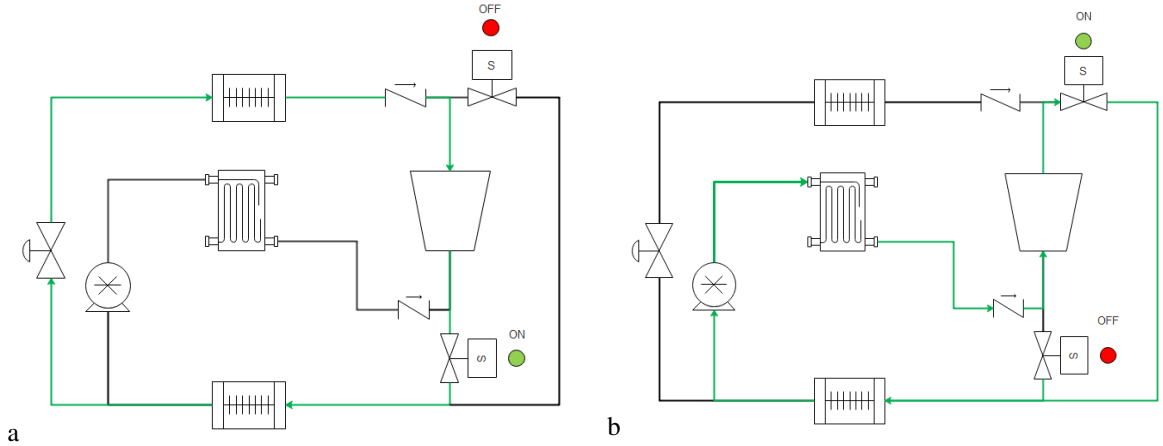

Figure 1: ReverCycle in MAC mode (a) and ORC mode (b)

2.2 Sizing

ReverCycle must acknowledge the cabin cooling needs of a medium size vehicle.
The nominal point for the air conditioning mode is defined as follows.

- The ambient temperature is set to 45 °C.
- The required cooling power is 6 kW.
- The condenser saturation pressure is set to 19.8 bar (abs) and the evaporator pressure is 4 bar (abs) according to standard operating values.
- The nominal condenser subcooling and evaporator superheating are set to 1 and 5 K, respectively.

The cycle thermodynamic points and compressor volumetric flow rate are calculated via a VBA code. The model is based on simple energy balances. The geometry of the heat exchangers is calculated using the Air Conditioning library [25] and the model boundary conditions are provided by the VBA model. The condenser and evaporator are modeled as micro-channel heat exchangers.

The design point of the ORC mode is the highway operation at 120 km/h. The chosen heat source is the engine coolant. The available heat flow rate is 13.4 kW and the coolant temperature is 105 °C with a mass flow rate of 0.8 kg/s. The ambient temperature is set to 20 °C, instead of 45°C for the MAC mode, since the ORC can be run only when MAC activation is not needed. The thermodynamic cycle is defined as follows.

- The boiler saturation pressure and condenser pressure are set to 30 and 10 bar, respectively.
- The nominal condenser subcooling and boiler superheating are set to 1 and 10 K, respectively.

The cycle thermodynamic points, turbine volumetric flow rate, and geometry of the heat exchangers are calculated similar to those in the air conditioning mode by coupling a VBA code with the Air Conditioning library. The condenser is modeled as a micro-channel heat exchanger and the boiler as a brazed plate heat exchanger. The net recovered mechanical power in the ORC mode is 0.98 kW.

Two components are mutualized, namely the scroll machine and MAC/ORC condenser. The scroll machine should be an off-the-shelf automotive scroll compressor; thus, the reversible machine is a SANDEN TRSA05 compressor. The MAC and ORC condensers are four-pass micro-channel heat exchangers with louvered fins. There are 64 fins at every 10 cm. The dimensions of the MAC condenser are 50 cm x 45 cm x 1.6 cm, while those of the ORC condenser are 62 cm x 45 cm x 2.2 cm.

The ORC condenser is larger and deeper as compared to the MAC but its dimensions are still in automotive standards. The ReverCycle condenser has the size of the ORC condenser.

3. METHODOLOGY

Heidrich and Krisch [26] emphasized that evaluating the fuel economy of an ORC on the design point is only half the truth. In real life operation, the ORC system will experience transient operation conditions. Waste heat recovery fuel economy has then to be assessed on the WLTC cycle (Figure 2) [27]. This global and harmonized standard allows determining vehicle fuel consumption as close as possible to the real driving conditions. The cycle is divided in four different phases simulating urban, suburban, rural and highway scenarios.

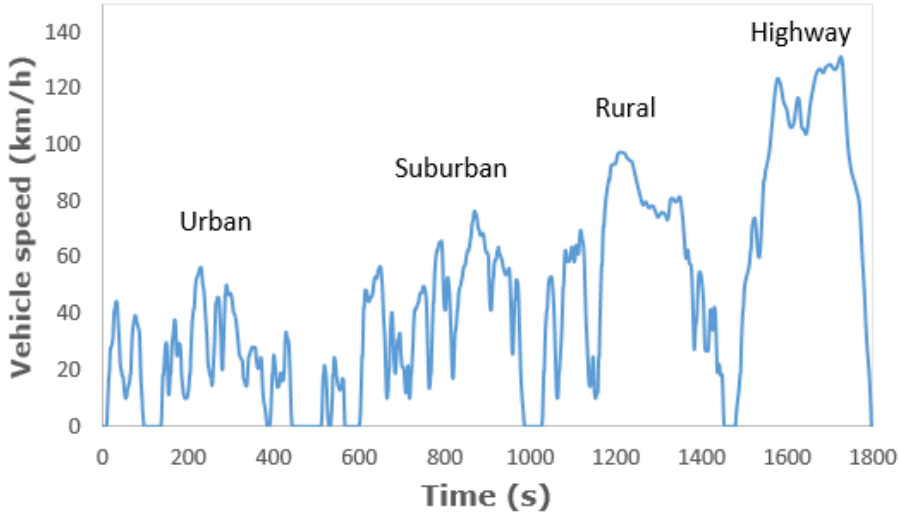

Figure 2: Vehicle speed profile on a WLTC cycle

In addition to that, Horst *et al*. [13] and Usman *et al*.[5] showed the importance of assessing the negative impact of the interaction between the ORC system and other vehicle systems.
A global vehicle model can estimate the fuel economy of ReverCycle in ORC mode on a WLTC cycle and study its interaction with the engine cooling circuit. The vehicle model is developed within the Dymola environment. The model is composed of three different modules (Powertrain model, Engine cooling circuit model, and ORC model) that are described in Section 3.1.
As shown in Figure 3, the global vehicle model allows the calculation of fuel economy in the ORC mode; however, to assess the fuel economy of ReverCycle, information regarding MAC activation time is required. ReverCycle can operate as ORC only if the MAC is not running. The annual averaged activation of the air conditioning system is assessed by coupling a cabin thermal model with a thermal comfort model. The two models are described in Section 3.2.

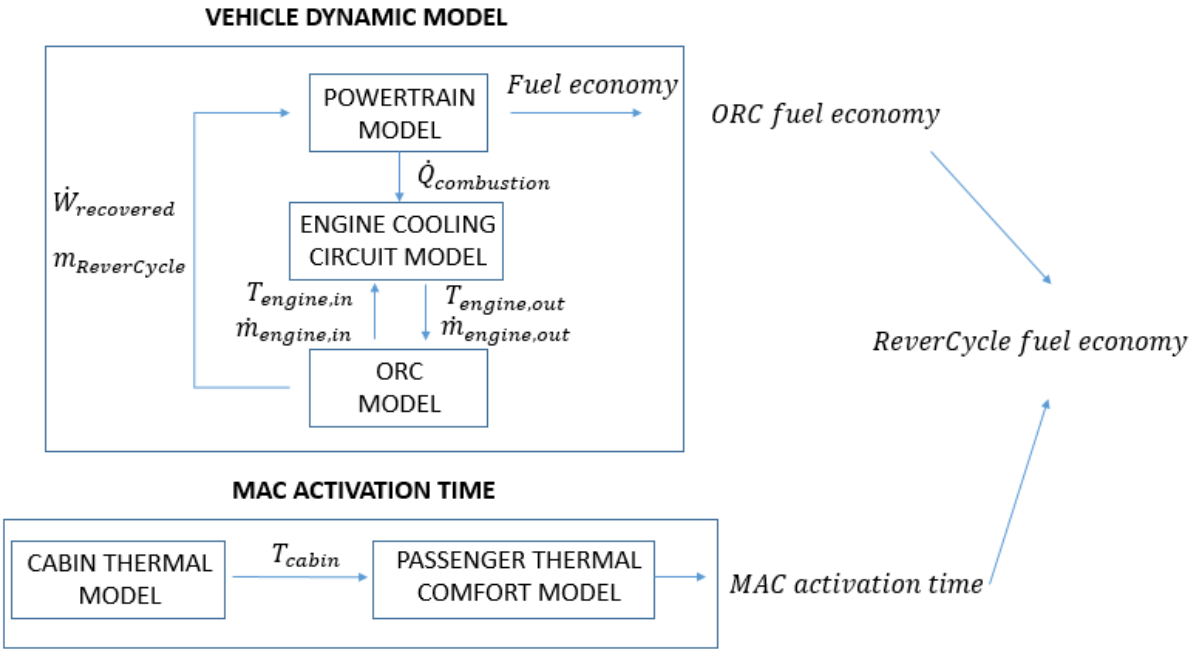

Figure 3: Methodology to assess ReverCycle fuel economy

3.1 Global vehicle model

3.1.1 Powertrain and engine thermal model

The powertrain model is based on the work of Mansour and Clodic [28]. The model, originally developed for a hybrid vehicle, is adapted to a conventional spark ignited engine vehicle. It enables the prediction of vehicle fuel consumption on a driving cycle imposed by the user. Engine and accessory consumptions are table based.

The engine thermal model is based on the PowerTrain library[29,30] where the engine power loss is based on an empirical correlation function of engine speed, ω, defined as

$$Power\ Loss = (Chem.energy - Mech.energy)(a\omega^2 + b\omega + c) \quad (1)$$

Where a = -5 10^{-8}, b = -7 10^{-5} and c= 0.84.

The calculated heat flow enters a thermal network, as shown in Figure 4, which calculates the heat flow while entering the engine cooling circuit capacitance.

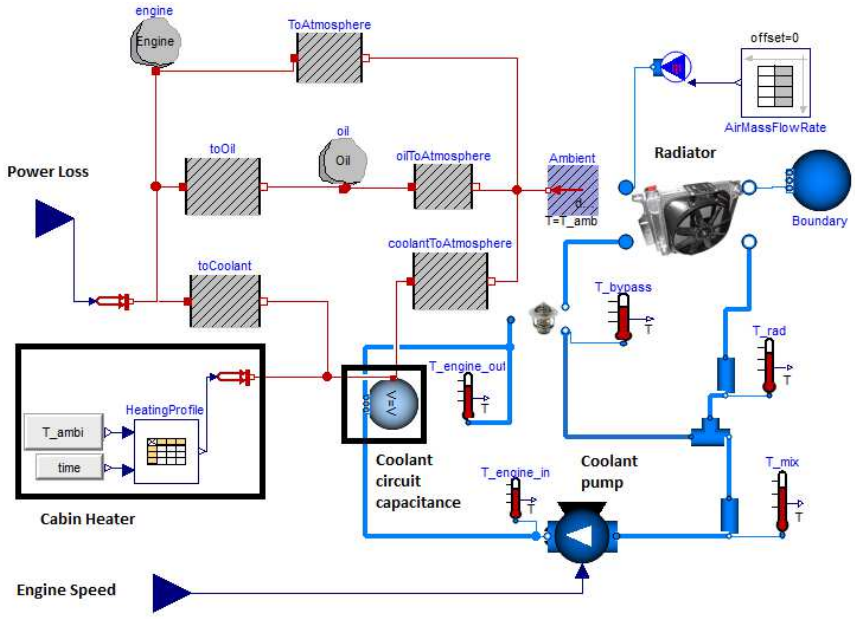

Figure 4: Engine thermal model and cooling circuit model

3.1.2 Engine cooling circuit model

The engine cooling system enables the engine to work at optimal conditions. It consists of a closed hydraulic circuit fed by a centrifugal pump coupled with the engine speed via a pulley-belt system. The basic architecture is composed of five main components, i.e., the pump, engine block, thermostat, radiator, and cabin heater. The cooling medium is a water/glycol mixture. The radiator rejects the coolant waste heat but during engine warm up, a radiator by-pass circuit is present to accelerate the rise in temperature. In traditional configurations, a wax thermostat manages the by-pass control.

The cabin heater is a smaller radiator used for cabin heating; this is a simple waste heat recovery application that enables passenger thermal comfort while exploiting the thermal losses in the engine.

The heat exchanger thermal power is table based. It is modeled as a power loss in the engine block capacitance. The cabin heating need on a WLTC cycle is calculated with the method proposed by Mansour *et al.* [31].

The higher inertia components, engine block and radiator control the dynamics of the engine cooling systems. The radiator is modeled with a lumped parameter approach where the coolant, air, and wall capacitances are considered. The following system of differential and algebraic equations defines the radiator model:

$$\frac{dm_{cool}}{dt} = \dot{m}_{cool,in} - \dot{m}_{cool,out} \tag{2}$$

$$m_{cool} = \rho_{cool} V_{cool} \tag{3}$$

$$m_{cool} c_{cool} \frac{dT_{cool}}{dt} = \dot{m}_{cool,in}\, c_{cool,in} T_{cool,in} - \dot{m}_{cool,out}\, c_{cool,out} T_{cool,out} + - AU_{cool}\left(\frac{T_{cool,in} + T_{cool,out}}{2} - T_{rad,wall}\right) \tag{4}$$

$$\dot{m}_{air,in} = \dot{m}_{air,out} = \rho_{air} A_{rad} v_{air} \tag{5}$$

$$0 = \dot{m}_{air}\, c_{air}\left(T_{air,in} - T_{air,out}\right) - AU_{air}\left(\frac{T_{air,in}+T_{air,out}}{2} - T_{rad,wall}\right) \tag{6}$$

$$m_{wall} c_{wall} \frac{dT_{wall}}{dt} = AU_{cool}\left(\frac{T_{cool,in}+T_{cool,out}}{2} - T_{rad,wall}\right) - AU_{air}\left(\frac{T_{air,in}+T_{air,out}}{2} - T_{rad,wall}\right) \tag{7}$$

Table 1 : Radiator model parameters

Component	Parameter	
Coolant	U_{cool}	2000 W/m^2/K
	HTA_{cool}	0.8 m^2
	V_{cool}	0.002 m^3
Wall	m_{wall}	6 kg
	c_{wall}	880 J/kg/K
Air	U_{air}	$20 + 10\left(\rho_{air} v_{air}\right)^{0.75}$ W/m^2/K [32]
	HTA_{air}	5 m^2

Table 1 summarizes the main parameters of the radiator model. An important model variable is v_{air}, the air speed at the radiator inlet. The experimental data provided by Ap [33] are used to derive the air speed at the radiator inlet from the vehicle speed.
The coolant circuit inside the engine block is modeled as a capacitance receiving heat from the engine thermal model.
Feed pump and thermostat dynamics are fast and their model can be of steady state type. Experimental data, provided by Groupe PSA, suggest a linear relationship between the feed pump flow rate and engine speed.
The wax thermostat is modeled as a three-way valve where the opening and closure behaviors consider the temperature hysteresis.
The dynamic model is then validated based on experimental results, provided by Groupe PSA, on a 1000 s dynamic driving cycle. The comparison of coolant temperatures between experimental results and the simulation is shown in Figure 5.
The temperature rise at the engine outlet (Figure 5b) is faster during the experimental test than that in the simulation. A possible reason is the engine model, which is table based and does not consider combustion inefficiencies at cold start. Slower temperature rise (Figure 5b) in the simulation implies a delay in thermostat opening and radiator outlet temperature (Figure 5a). The maximum absolute error for the engine outlet temperature is 16 K whereas that for the radiator outlet temperature is 22 K. The waste heat of the engine coolant is available for recovery only when the thermostat is open. Therefore, the impact of the modeling error is a reduced period for waste heat recovery, compared to real life conditions.

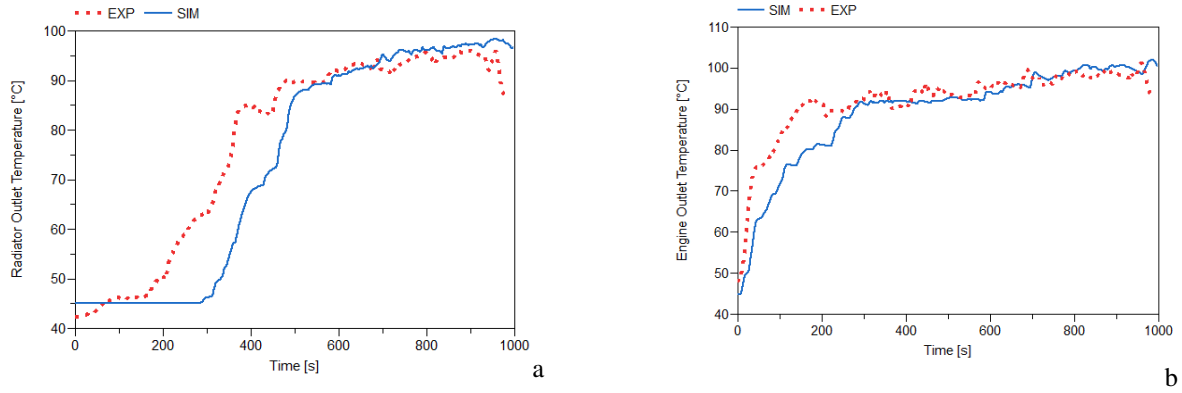

Figure 5: Dynamic model validation: (a) Radiator outlet temperature and (b) Engine outlet temperature.

3.1.3 ORC model

The ReverCycle ORC mode is modeled using the ThermoCycle library [34]. The working fluid properties are calculated via the Coolprop library [35].
Heat exchangers are simulated as finite volume counter current heat exchangers. The energy and mass balance for one fluid cell are expressed by:

$$V\left(\frac{\partial\rho}{\partial h}\frac{dh}{dt}+\frac{\partial\rho}{\partial p}\frac{dp}{dt}\right)=\dot{m}_{in}-\dot{m}_{out} \quad (8)$$

$$\rho V\frac{dh}{dt}=\dot{m}_{in}(h_{in}-h)-\dot{m}_{out}(h_{out}-h)+AU\,(T_{wall}-T)+V\frac{dp}{dt} \quad (9)$$

The energy balance for the wall cell is expressed by:

$$m_{wall}c_{wall}\frac{dT_{wall}}{dt}=AU_{ref}\left(T_{ref}-T_{wall}\right)-AU_{cool}(T_{cool}-T_{wall}) \quad (10)$$

The heat transfer area and nominal heat transfer coefficients, U_{nom}, in Table 2 are retrieved from the sizing phase results. The heat transfer coefficients, U, depend on the mass flowrate [34].

$$U=U_{nom}\left(\frac{\dot{m}}{\dot{m}_{nom}}\right)^{0.8} \quad (11)$$

Pressure losses in the heat exchangers are neglected. A local pressure drop is introduced at the expander exit. The pressure drop is a linear correlation with the volumetric flowrate with a coefficient of 1.152 10^{-7}.

The pump is modeled as a volumetric pump with a displacement of 1.5 cc. The definition of isentropic efficiency, η_{is}, and mechanical efficiency, η_{mech}, enables us to determine the mechanical work of the pump.

The expander model is based on the semi-empirical approach proposed by Lemort *et al.* [36]. The built-in volume ratio of the expander, BVR, is 1.9. The BVR is calculated by analyzing a 2D scanner image of the Sanden TRSA05 scrolls. Figure 6 shows the conceptual scheme of the model. A fictitious envelope represents the metal mass of the expander and its thermal inertia.

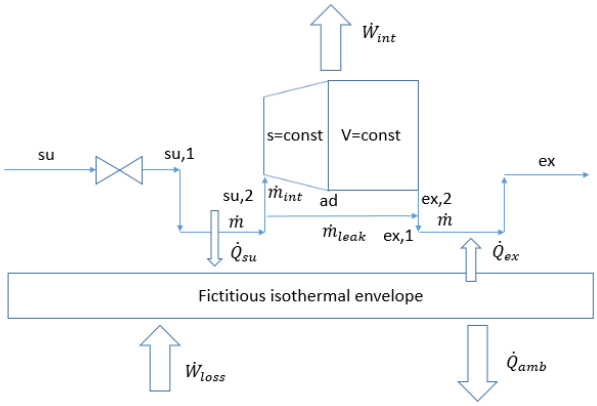

Figure 6: Conceptual scheme of the expander model [36]

Five empirical parameters consider the different physical phenomena occurring in the expander. The heat transfer coefficients, AU_{amb}, AU_{su}, and AU_{ex}, respectively, describe the heat transfer losses to the environment, at the expander suction, and the expander exit. The surface A_{leak} and the diameter d_{su} enable the calculation of mass leakage between the scroll chambers and the suction pressure drop. Two constant mechanical efficiencies consider the internal losses of the expander, η_{mech}, and the transmission losses, η_{trans}. The model parameters, except the BVR, are calibrated on internally available experimental results of a Sanden TRSA05 expander. The expander model predicts the recovered work within a 10% error bar, which is in line with others Lemort's model validation results[36–38]. Table 2 presents all ORC model parameters.

Table 2 : ORC model parameters

Component	Parameter	
Boiler	$U_{l,nom}$	200 W/m²/K
	$U_{tp,nom}$	4000 W/m²/K
	$U_{v,nom}$	70 W/m²/K
	HTA_{ref}	1.4 m²
	HTA_{cool}	1.4 m²
	$U_{cool,nom}$	4000 W/m²/K
	$\dot{m}_{ref,nom}$	0.06 kg/s
	$\dot{m}_{cool,nom}$	0.66 kg/s
Condenser	$U_{v,nom}$	75 W/m²/K
	$U_{tp,nom}$	4000 W/m²/K
	$U_{l,nom}$	500 W/m²/K
	HTA_{ref}	0.6 m²
	HTA_{air}	8.7 m²
	$U_{air,nom}$	150 W/m²/K
	$\dot{m}_{ref,nom}$	0.06 kg/s
	$\dot{m}_{air,nom}$	0.8 kg/s
Pump	η_{is}	70%
	η_{mech}	90%
Expander	BVR	1.9
	m_{exp}	5 kg
	AU_{amb}	0.3 W/K
	AU_{su}	23 W/K
	AU_{ex}	0.1 W/K
	A_{leak}	$1.6\ 10^{-6}$ m²
	d_{su}	$6.47\ 10^{-3}$ m
	η_{mech}	98 %
	η_{trans}	90 %

3.1.4 ORC model validation

A validation of the ThermoCycle library has been provided by their developers in [39]. However, it was preferred to carry out a validation of the ORC model on dynamic conditions closer to the ReverCycle application.

Therefore, the validation of the ORC model is based on an experimental test performed on the ORC circuit of the ReverCycle proof of concept. The test bench is used to simulate the working conditions of an ORC in a conventional vehicle running a WLTC at an ambient temperature of 16°C.

Figure 7 show the test bench layout. Refrigerant R134a is the ORC working fluid. Table 3 presents the test bench main equipment. The heat exchangers and expander selection is based on the ReverCycle design, while the diaphragm pump used in this test bench is too bulky to fit the vehicle available free volume. The pump motor and the expander generator are connected to two inverters, which allow controlling the rotational speeds of the machines. Table 4 summarizes the instrumentation setup.

The engine and engine coolant circuit have been simulated via a closed loop circuit made of a variable speed pump, a 12 kW electric heater and a 800 liters water tank at atmospheric pressure.

In order to avoid boiling conditions in the water tank, the circuit temperature is fixed to 92°C.

This implies a performance reduction for the ORC, compared to an automotive application, since normally the engine coolant temperature is around 100°C.

The engine cooling circuit model is used to determine the evolution of the mass flow rate at the boiler inlet. In order to protect the electric heater from overheating, a minimum mass flow rate of 0.1 kg/s has to be ensured.

Figure 8 shows the final mass flowrate profile imposed to the pump.

The 800 l water tank allows keeping a constant outlet temperature during the WLTC simulation.

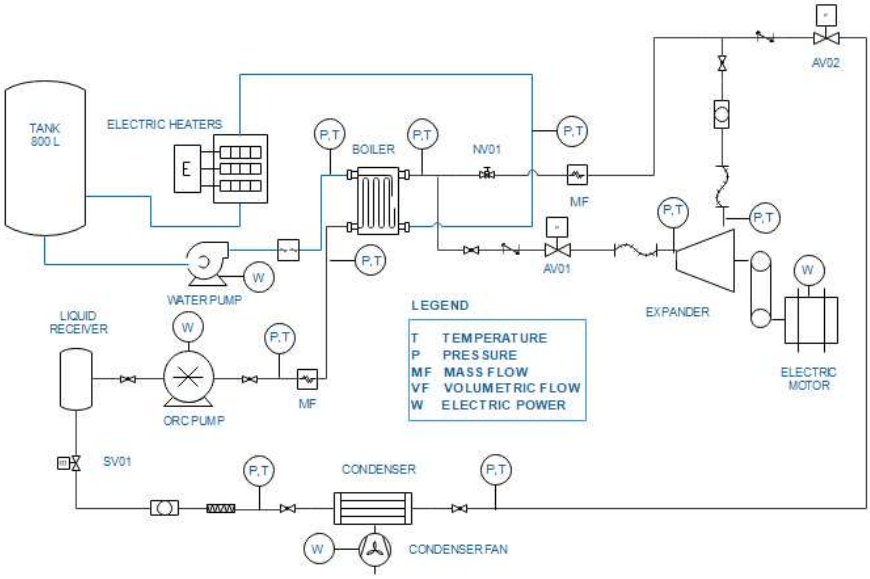

Figure 7: ORC test bench layout

Table 3: Main components of the ORC test bench

Component	Reference
Expander	SANDEN TRSA05
Boiler	SWEP B12MTx50
Condenser	FrigAir Spa 0818.2031
Fan	S&P HRT/4-400 BPN
ORC pump	Wanner G13XKSTHFEPA

Table 4: Instrumentation Setup

Sensor	Location	Accuracy
Temperature	ORC circuit	+/- 0.16 K
Pressure	ORC circuit	+/- 0.1% FS [0-30 bar]
Volumetric Flow Rate	Auxiliary water circuit	+/- 0.4%
Mass Flow Rate	ORC circuit	+/- 0.5%
Electric Power	Expander	+/- 1%
Electric Power	ORC Pump	+/- 0.8% FS [0-750 W]

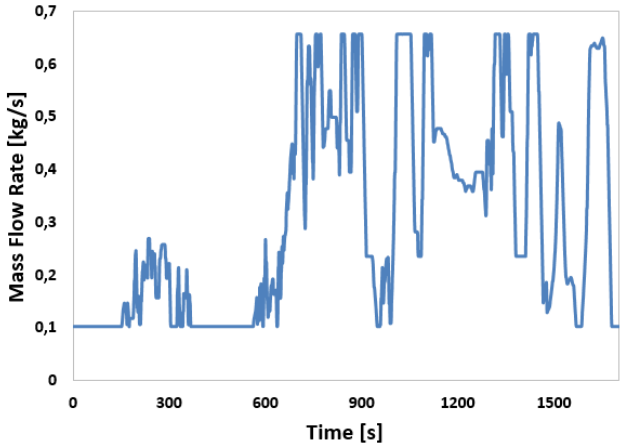

Figure 8: Pump mass flowrate

The inverters impose a speed profile to the pump and expander. The speed profiles, see Figure 9, reproduce the engine behaviour over a WLTC cycle.

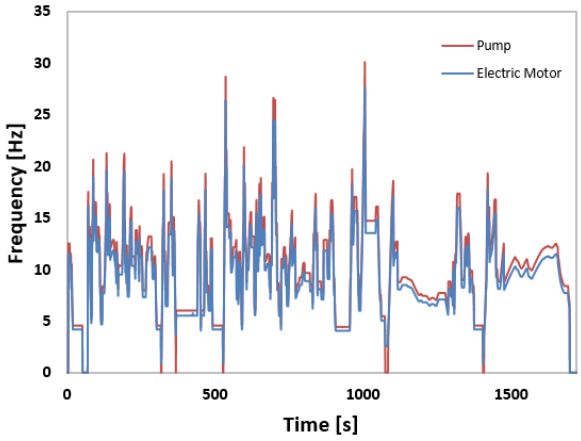

Figure 9: Pump and expander frequency profile

In the ORC model, a fixed electric efficiency of 90% is imposed to the expander generator, while the electric power of the pump is simulated via the following equation:

$$W_{el} = W_{hydraulic}\,(1 + a) + W_0 \tag{12}$$

Where a = 0.165 and W_0 is equal to 36.17.
The ORC model is able to represent the boiler thermal power, see Figure 10, with a NRMSD of 5% and the expander electric power, see Figure 11, with a NRMSD of 11 %. Figure 12 shows that the simulation model is not accurate in the evaluation of the inlet and outlet pressure with a NRMSD of respectively 6% and 8%. The error on the expander pressure ratio affects the calculation of the generated power. The difference between experimental and simulation results for the inlet and outlet temperatures, see Figure 13, is probably related to the position of the temperature sensors. The sensors are not close to the expander body and the lines are not thermally insulated, so heat losses are present.
Furthermore, the lower performance of the expander model probably depends on two simplifications: a constant leakage area model and the use of fixed efficiencies to describe the behavior of the generator and the transmission system. The absence of a torque sensor on the expander shaft has not allowed a thorough investigation.

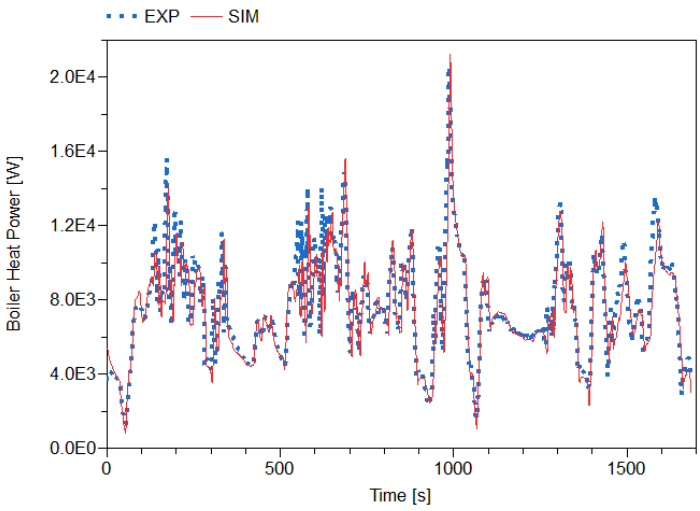

Figure 10: ORC model transient validation on a WLTC: boiler thermal power

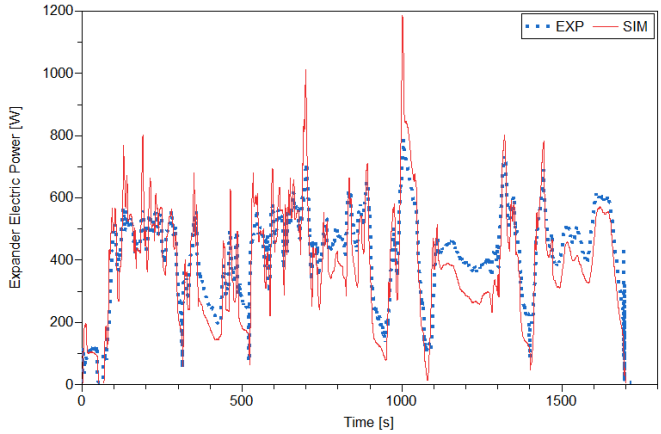

Figure 11: ORC model transient validation on a WLTC: expander electric power

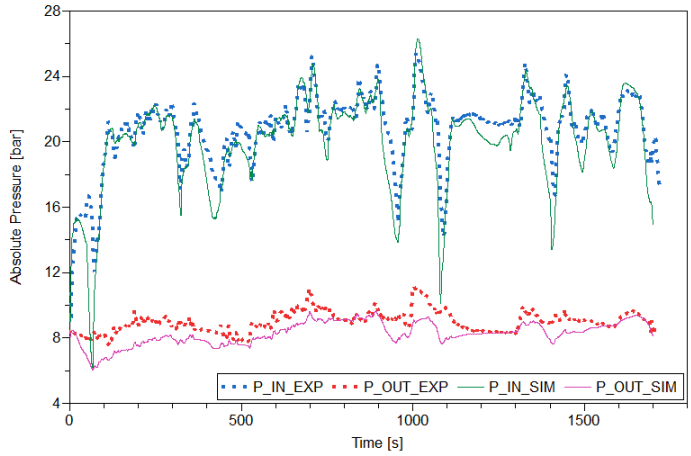

Figure 12: ORC model transient validation on a WLTC: expander pressures

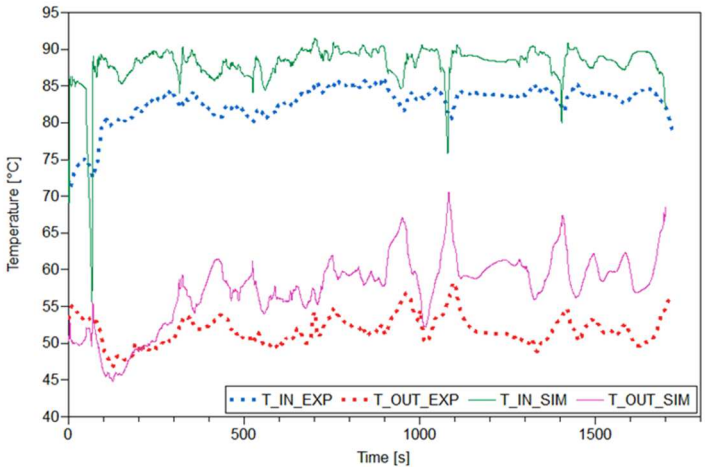

Figure 13: ORC model transient validation on a WLTC: expander temperatures

The expander isentropic efficiency is defined as:

$$\eta_{exp,is} = \frac{\dot{W}_{exp,el}}{\dot{m}_{R134a}(h_{exp,in} - h_{exp,out,is})} \quad (13)$$

Figure 14 shows the evolution of this important performance indicator during the test. The experimental work of Dumont *et al* [37] has shown that the isentropic efficiency of an automotive electric scroll

compressor converted into an expander is of the order of 40-75% at low pressure ratios. In the ReverCycle test bench, the expander is coupled to the generator shaft via a pulley-belt system which is less efficient than a direct mechanical connection as in the electric scroll compressor tested in [37]. This causes additional mechanical losses. However, considering the strong dynamics of the cycle, the expander is showing relatively high efficiencies.

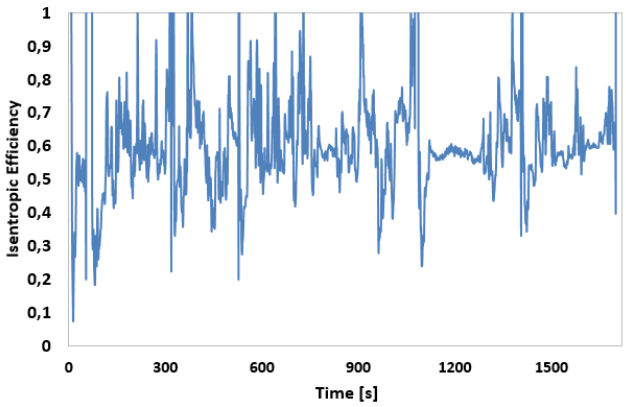

Figure 14: Expander measured isentropic efficiency

ORC cycle efficiency is evaluated, given by

$$\eta_{cycle} = \frac{\dot{W}_{net}}{\dot{Q}_{hot\ source}} \tag{14}$$

The measured ORC efficiency, averaged over the simulated WLTC cycle, is 3.3 %. The ORC model predicts an averaged efficiency of 3.1%, thus the relative error is 6%. Considering the low temperature level of the heat source (92°C) and the highly dynamic working conditions of the test, the measured efficiency is a promising result for waste heat recovery from the engine coolant.

3.2 MAC activation time

The procedure used to estimate the MAC activation time is similar to that developed by Johnson [40]; it is based on the thermal comfort mode proposed by Fanger [41]. Figure 15 shows the flowchart of the comfort model. The main difference between this work and that by Johnson [40] is in the calculation of the soak temperature. In this study, the mono-zone cabin thermal model developed by Benouali [42] is used instead of an empirical correlation.

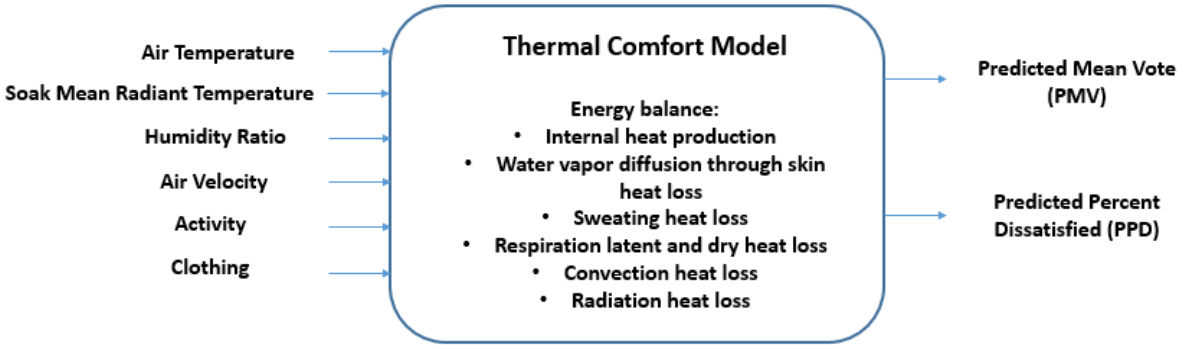

Figure 15: Comfort model flow chart

3.2.1 Cabin Thermal Model

The cabin thermal model is a simplified lumped-capacitance model based on three thermal capacitances, namely the cabin air, vehicle body, and glass. Figure 16 illustrates the electro-thermal analogy of the model.
A system of ordinary differential equations describes the temporal evolution of the three thermal nodes.

$$\left(\sum_i m_i c_i\right)\frac{dT_{car}}{dt} = AU_{car_{int}}(T_{ac} - T_{car}) - AU_{car_{ext}}(T_{car} - T_{ext}) + I_{car\_absorb}A_{car} \tag{15}$$

$$\left(\sum_j m_j c_j\right)\frac{dT_{glass}}{dt} = AU_{glass_{int}}(T_{ac} - T_{glass}) - AU_{car_{ext}}(T_{glas} - T_{ext}) + I_{glas\_absorb}A_{glas} \tag{16}$$

$$(m_{ac}c_{ac} + m_{mi}c_{mi})\frac{dT_{ac}}{dt} = c_{inf}.\dot{m}_{inf}(T_{out} - T_{ac}) - AU_{car_{int}}(T_{ac} - T_{car}) - AU_{glass_{int}}(T_{ac} - T_{glass}) + I_{trans}.A_{glass} \tag{17}$$

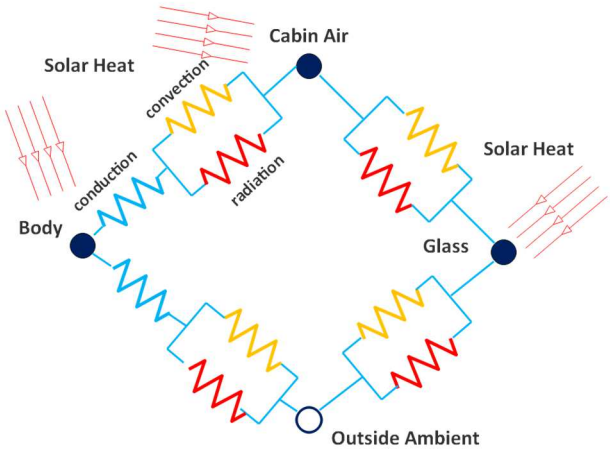

Figure 16: Electro-thermal analogy of the cabin thermal model

The simulation results were validated on the experimental data by Marcos *et al.* [43]. The authors performed different tests on a midsize sedan. The first test was performed on a vehicle located outdoors under sun irradiance, as shown in Figure 17, and without passengers. This test was used to validate the model of Benouali in soak conditions.

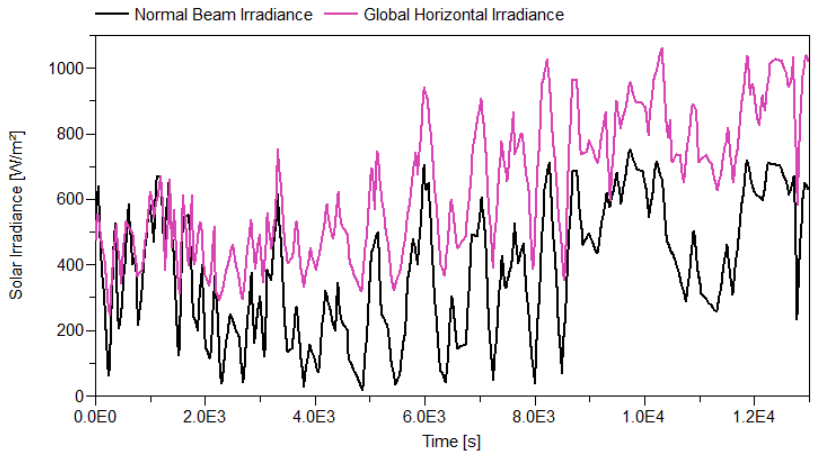

Figure 17: Test: sun irradiance [43]

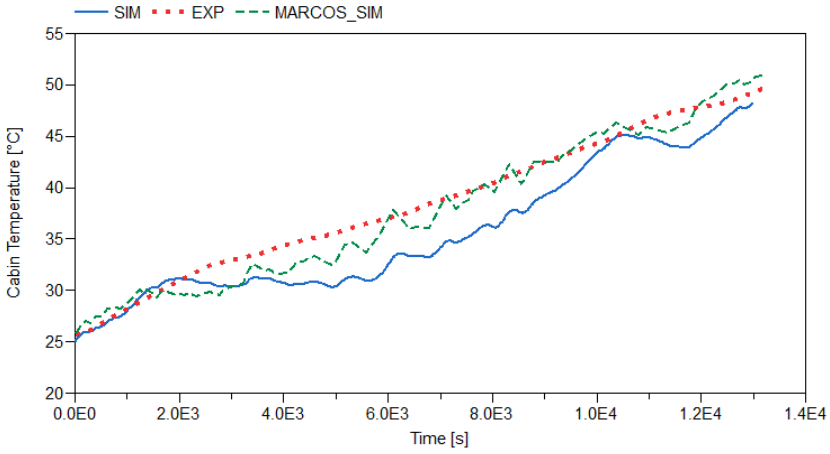

Figure 18: Cabin temperature evolution: Marcos model (green), Benouali model (blue), test [43] (red)

The Benouali model exhibited similar results to the Marcos model (see the comparison in Figure 18) even if the maximum absolute error was higher (4 K in comparison to 2 K).

3.2.2 Results

The first step of the calculation procedure to assess the MAC activation time consists of selecting a climatic region and the corresponding weather data from a database [44]. The weather data are selected exclusively during the 7am–8pm interval, wherein the time step is one hour. The cabin thermal model calculates the cabin soak temperature for each time step. This information is the main input for the thermal comfort model developed by Fanger [41], which is used to calculate the predicted percentage of people dissatisfied (PPD) by the comfort condition in the cabin. A dissatisfied driver will turn on the MAC system.

Table 5: MAC activation time for various climatic conditions

City	MAC activation time
Paris	21%
Moscow	16%
Valencia	41%
Brasilia	59%

A yearly simulation is performed and the average MAC activation time for different cities is presented in Table 5. Each city represents a specific climatic region. Paris represents an oceanic climate in the Köppen climate classification, Valencia a Mediterranean climate, Brasilia a tropical climate, and Moscow a humid continental climate.
Figure 19 shows the temperature occurrence frequency in the four cities.

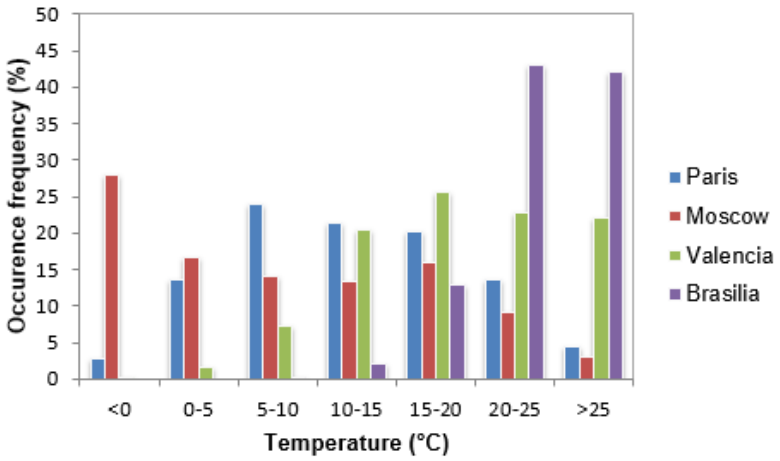

Figure 19: Temperature occurrence frequency for four different climatic regions

4 RESULTS

ReverCycle has a simple mechanical architecture where the ORC pump and expander speeds depend on the speed of the engine shaft. This mechanical system then has two parameters to optimize, namely the speed ratio between the pump and the engine and that between the expander and the engine. We need to calculate the optimal speed ratios before assessing the ReverCycle fuel economy.

4.2 Optimal speed ratios in ORC mode

The reference speed ratios are the ones calculated at the design point. Positive and negative variations of 40% are applied to each speed ratio, thereby yielding a nine-point test matrix (see Table 6).
A WLTC cycle is run for each of the nine points and the average ORC cycle efficiency is evaluated, given by equation (14).
The ambient temperature and initial engine cooling circuit temperature are set to 20 and 85 °C, respectively.
Table 6 identifies the reference condition as the optimal solution; however, the results do not consider the effect of vapor quality at the expander inlet.
The expander simulation model does not consider the negative effect of liquid droplets inside the expander. Scroll expander can tolerate liquid droplets; however, Figure 20 demonstrates that most of the speed ratios imply a permanent two-phase expansion with low vapor quality.
The only acceptable solutions are the ones that involve a speed ratio of 0.6 between the pump and the engine. A speed ratio of 0.24 between the expander and the engine is too low for the correct operation of the machine. At low rotational speeds, mass leakages are important because the low centrifugal forces do not ensure a correct sealing effect between the scroll chambers. The expander model does not consider this phenomenon.
The final choice is then a speed ratio of 0.6 between the pump and the engine and a speed ratio of 0.4 between the expander and the engine.

Table 6: ORC average cycle efficiency as a function of speed ratios

	Pump/Engine 0.6	**Pump/Engine 1**	**Pump/Engine 1.4**
Expander/Engine 0.24	4.2 %	4.8 %	4.1 %
Expander/Engine 0.4	2.5%	5 %	4.8 %
Expander/Engine 0.56	2 %	3.9 %	4.2%

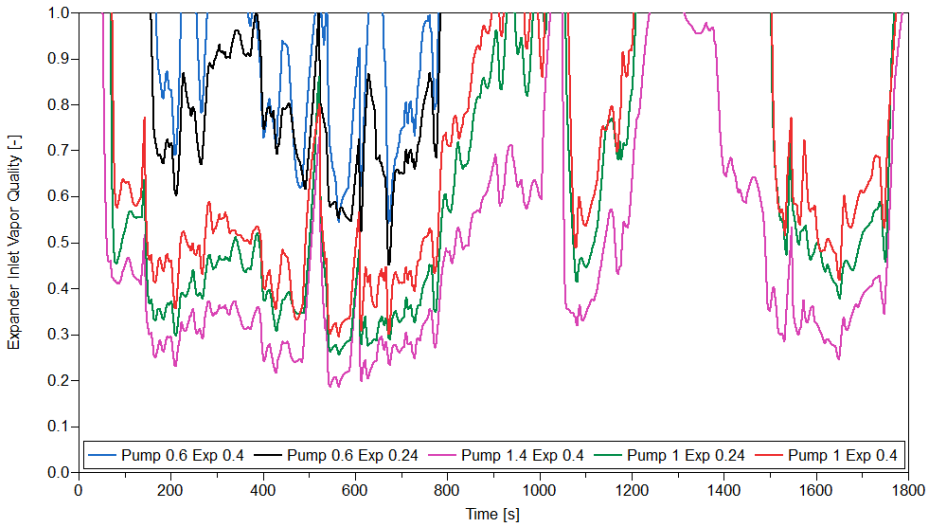

Figure 20: Working fluid vapour quality at expander inlet for different speed ratios

4.3 ReverCycle fuel economy

The MAC activation time calculation has provided important information on the ORC mode availability. The next questions involve ReverCycle fuel economy and Waste Heat Recovery (WHR) potential lost due to the absence of full ORC mode availability. The global vehicle model provides the answer.

The reference simulation is a WLTC cycle. The parameters are the initial engine cooling circuit temperature and ambient temperature. The engine cooling circuit temperature can be initialized at ambient temperature (cold start) or 85°C (hot start). The considered ambient temperature range is 0–30 °C. Below 0 °C, the totality of the engine coolant waste heat is necessary for cabin heating. Above 30 °C, MAC is always turned on. The temperature range is then divided in six 5 K temperature ranges and six average temperatures are defined. A WLTC cycle is run for each of the six average temperatures with a cold start and hot start initialization. The ORC model evaluates the net recovered mechanical power (see Figure 21). The net recovered mechanical power enables the identification of the net torque added to the engine by the expander belt. The new engine efficiency, owing to a different working point on the engine map, enables the estimation of the fuel economy.

Each simulation is weighted for its yearly occurrence to calculate the WHR potential over one year. ReverCycle fuel economy is calculated similarly, but each temperature range simulation is additionally multiplied by the ORC availability.

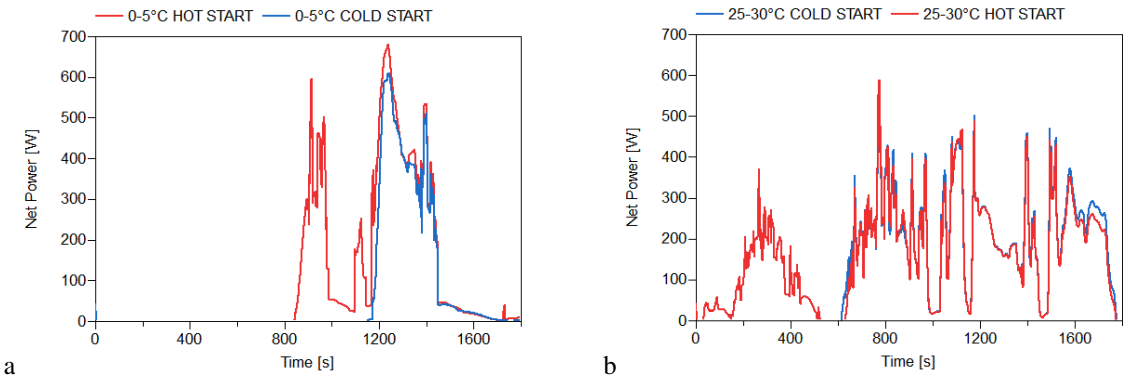

Figure 21: ReverCycle net power production for 0–5 °C ambient temperature range (a) and 25–30 °C (b)

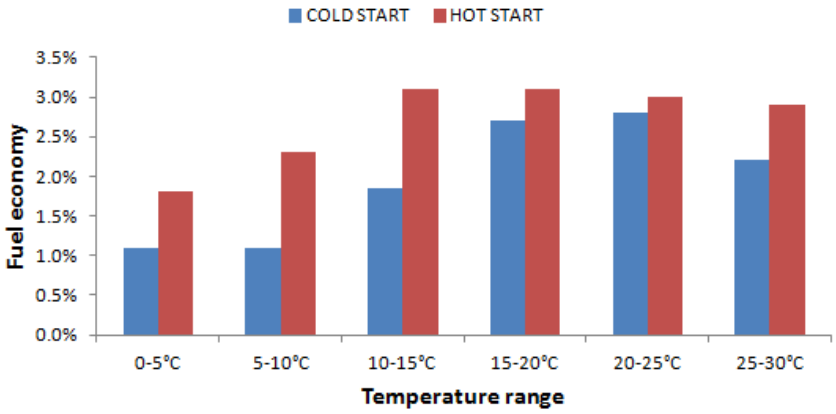

Figure 22: ReverCycle fuel economy for different ambient temperature ranges

Figure 22 shows the evolution of fuel economy at different ambient temperatures. The peak efficiency is observed around 15 °C. The peak is due to the two opposite effects depending on the ambient temperature, i.e., ORC efficiency and waste heat availability. ORC efficiency decreased with the ambient temperature, while waste heat availability increases mainly because of the cabin heater demand. The thermal power demand is lower at warm ambient temperatures. Figure 23 shows the influence of ambient temperature on ORC efficiency and waste heat availability. The peak position of the normalized net energy recovered (Figure 23) is different from the peak of fuel economy (Figure 22). This difference is due to a nonlinear relationship between the added torque to the engine and the corresponding fuel economy.

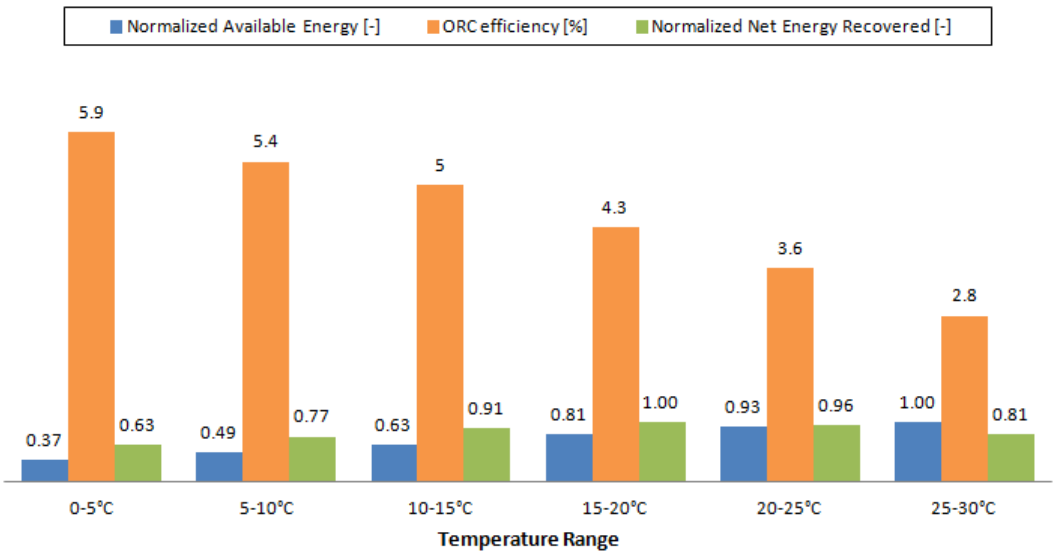

Figure 23: Influence of ambient temperature on ORC efficiency and waste heat availability

Table 7: ReverCycle fuel economy for different climatic conditions

City	HOT START Fuel economy	COLD START Fuel economy
Paris	2%	1.3%
Moscow	1.65%	1.05%
Valencia	1.68%	1.22%
Brasilia	1.13%	1%

Table 7 presents the results for the four different climatic regions. Paris offers the best climatic conditions to ReverCycle, which shows the highest fuel economy. ReverCycle fuel economy, in hot climatic regions like Brasilia and Valencia, is strongly affected by the MAC activation time.
In Paris and Moscow, the reversible MAC/ORC system loses approximately 25% of the ORC waste heat recovery potential owing to MAC activation time. In Valencia and Brasilia, this loss amounts to 43% and 58% of the ORC waste heat recovery potential due to the higher MAC activation time, respectively. Therefore, ReverCycle is an interesting solution for cold or mild climatic regions like the ones of Moscow and Paris.

Table 7 highlights a limit for waste heat recovery in the engine coolant. At cold start condition, waste heat recovery is possible only after engine warm up with a consequent impact on the achievable fuel economy, compared to the hot start condition. An interesting solution is to use the waste heat in the exhaust gases to reduce the engine warm up time. This would produce two positive effects on the fuel economy. First, decreasing the engine warm up time reduces fuel consumption [45]. Second, the increase of ReverCycle fuel economy at cold start conditions.

4.4 ReverCycle versus separated cycles

Revercycle MAC mode design respects automotive standards. Thus, when ReverCycle operates in MAC mode, no important performance loss is expected compared to a separated MAC. The selected compressor/expander is a mechanical scroll compressor. This is an initial choice due to the simplicity of the mechanical architecture. The urgent need to reduce vehicle consumption is forcing car manufacturers to improve MAC efficiency. Compressor electrification is a solution [46]. Electric, variable speed, scroll compressors are gaining interest in the automotive sector due to their higher

efficiencies compared to piston compressors. Therefore, the final choice for ReverCycle may be a reversible electric scroll machine.

In the ORC mode, Revercycle has a lower availability compared to a separated ORC.
In a climatic region like Paris, the advantage of ReverCycle in comparison to a separated ORC, recovering heat from the engine coolant, is important. Here, the ReverCycle fuel economy is 2% while the separated ORC fuel economy, calculated with our simulation model, is 2.4%. Both values of fuel economy take into account the negative effect of the added weight into the vehicle of the WHR system. The powertrain model, section 3.1.1, is used to estimate the impact.
The added weight of the components of the separated ORC is much more important (Figure 24). The added weight for the expander, which is considered in Figure 24, is the one of the SANDEN TRSA05 compressor. The boiler and the condenser weights are calculated via the Air Conditioning Library [25] (assuming they are aluminum made). ReverCycle ORC pump technology is not decided yet. The provided value is an estimation based on a gear pump model.

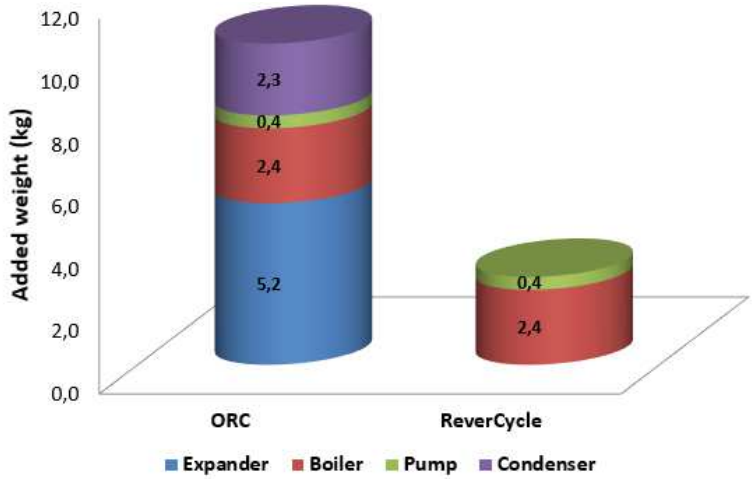

Figure 24: Added weight comparison: ORC vs ReverCycle

The separated ORC add to the vehicle an additional mass of 10 kg. This additional mass is causing a reduction of 0.2% of fuel economy. In other words, without taking into account the negative effect of the added mass, the separated ORC fuel economy in Paris would be around 2.6%. The influence of the added mass of ReverCycle components on fuel economy is almost negligible.
In a climatic region like Paris, it may be more interesting to develop a solution like ReverCycle instead of a separated ORC recovering heat from the engine coolant. The cost reduction due to the limited number of components is more interesting than increasing fuel economy from 2% to 2.4%.
A separated RC/ORC, recovering heat from the exhaust gases, has a higher fuel economy gain compared to ReverCycle. The fuel economy on a WLTC is estimated to be 3-4% depending on the architectures and the impact of cold start is limited [17]. The estimated weight is 10-15 kg.
Embedding a separated RC/ORC into a vehicle implies adding four components (pump, boiler, expander, condenser); in the case of ReverCycle, there are two added components (pump, boiler). Owing to the reduction in components, ReverCycle is not only a lighter solution than a RC/ORC but also cheaper.
In addition, it is noteworthy to mention that ReverCycle working fluid is the standard MAC refrigerant. There is then no need for validation of the working fluid, which can be quite complicated in the automotive sector.
It is difficult to accurately evaluate the cost of components because the available cost correlations are not reliable [47]. Furthermore, information in this sector is confidential. Thus, cost and payback time estimation are not performed in this study and it is then not possible to prove that ReverCycle has a faster payback time. Moreover, it is hard to anticipate the car manufacturers' choice, payback time is not the only argument, system compactness, ease of integration and reliability play a major role too.

ReverCycle meets all these needs, the further development of the solution and the realization of an embedded prototype will provide more insight on its potential.

5 CONCLUSIONS

This simulation study is the first stage in the development process of ReverCycle. ReverCycle is a reversible MAC/ORC system embedded in a light duty vehicle. The ORC is recovering waste heat in the engine coolant. Fuel economy is estimated via a global vehicle model. The ORC module has been validated with experimental results. The maximum measured ORC net efficiency on a dynamic cycle is 3.3%. Validation on experimental results has shown a NRMSD between 5% and 11% for the main ORC variables (pressures, temperatures and electric powers).The present work enables the quantification of the fuel economy of this reversible system that is, in Paris, between 1.3% and 2%. Embedding a separated ORC, instead of ReverCycle, would increase the maximum fuel economy from 2% to 2.4%. However, ReverCycle provides a consistent weight reduction due to the mutualization of two of the four ORC cycle components with the vehicle MAC system. An important cost reduction is also expected. In hotter climatic regions, like in Brasilia and Valencia, the interest in a solution like ReverCycle is less evident. The high MAC activation time is limiting the fuel economy of ReverCycle compared to a separated ORC.
The next step of the study is to validate the technical feasibility of the concept by finalizing the testing phase of the proof of the concept.
A further step is the introduction of a third operating mode, i.e., the ejector refrigeration cycle (ERC). This third mode could provide further fuel economy benefits by reducing the mechanical power required to cool the cabin [48,49].

ACKNOWLEDGMENT

This work was done in collaboration with Groupe PSA - Technical Center of Vélizy, France. The authors would like to thank “Groupe PSA” for their support.

NOMENCLATURE

A	Surface	[m^2]
AU	Thermal Conductance	[WK^{-1}]
c	Specific Heat Capacity	[$Jkg^{-1}K^{-1}$]
d	Diameter	[m]
h	Specific enthalpy	[Jkg^{-1}]
I	Solar Irradiance	[Wm^{-2}]
m	Mass	[kg]
$\dot{m}$	Mass flow rate	[kg/s]
p	Pressure	[Pa]
$\dot{Q}$	Thermal Power	[W]
s	Specific entropy	[$Jkg^{-1}K^{-1}$]
t	Time	[s]
T	Temperature	[°C]
U	Heat Transfer Coefficient	[$Wm^{-2}K^{-1}$]
V	Volume	[m^3]
v	Speed	[ms^{-1}]
$\dot{W}$	Power	[W]

Greek symbols

η	Efficiency	[-]
ρ	Density	[kgm^3]
ω	Rotational speed	[rpm]

Acronyms

BMW	Bayerische Motoren Werke	
BVR	Built-in Volume Ratio	
ERC	Ejector Refrigeration Cycle	
HTA	Heat Transfer Area	[m^2]
MAC	Mobile Air Conditioning	
NRMSD	Normalized Root Mean Square Deviation	
ORC	Organic Rankine Cycle	
PPD	Predicted Percent Dissatisfied	
PSA	Peugeot Société Anonyme	
RC	Rankine Cycle	
VBA	Visual Basic for Applications	
WHR	Waste Heat Recovery	
WLTC	Worldwide Harmonized Light Vehicles Test Cycles	

Subscripts

absorb	Absorbed
ac	cabin air
ad	adapted
amb	Ambient
car	car body
cool	Coolant
el	Electric
ex	Exit
exp	Expander

ext	External
inf	Infiltration
int	Internal
is	Isentropic
l	Liquid
mi	interior mass
mech	Mechanical
nom	Nominal
rad	Radiator
ref	Refrigerant
su	Suction
tp	two phase
trans	Transmission
trans	Transmitted
v	Vapor

REFERENCES

[1] Stobart R, Weerasinghe R. Heat Recovery and Bottoming Cycles for SI and CI Engines - A Perspective. SAE Tech. Pap. Ser., 2010. doi:10.4271/2006-01-0662.

[2] Holmberg K, Andersson P, Erdemir A. Global energy consumption due to friction in passenger cars. Tribol Int 2012. doi:10.1016/j.triboint.2011.11.022.

[3] El Chammas R. Rankine Cycle for hybrid vehicles, simulation and design of a first prototype. PhD Thesis at Ecole des Mine de Paris, 2005.

[4] Zhou F, Joshi SN, Rhote-Vaney R, Dede EM. A review and future application of Rankine Cycle to passenger vehicles for waste heat recovery. Renew Sustain Energy Rev 2017. doi:10.1016/j.rser.2016.11.080.

[5] Usman M, Imran M, Yang Y, Park BS. Impact of organic Rankine cycle system installation on light duty vehicle considering both positive and negative aspects. Energy Convers Manag 2016. doi:10.1016/j.enconman.2016.01.044.

[6] Orr B, Akbarzadeh A, Mochizuki M, Singh R. A review of car waste heat recovery systems utilising thermoelectric generators and heat pipes. Appl Therm Eng 2016. doi:10.1016/j.applthermaleng.2015.10.081.

[7] Kempf N, Zhang Y. Design and optimization of automotive thermoelectric generators for maximum fuel efficiency improvement. Energy Convers Manag 2016. doi:10.1016/j.enconman.2016.05.035.

[8] Aghaali H, Ångström HE. A review of turbocompounding as a waste heat recovery system for internal combustion engines. Renew Sustain Energy Rev 2015. doi:10.1016/j.rser.2015.04.144.

[9] Saidur R, Rezaei M, Muzammil WK, Hassan MH, Paria S, Hasanuzzaman M. Technologies to recover exhaust heat from internal combustion engines. Renew Sustain Energy Rev 2012;16:5649–59. doi:10.1016/j.rser.2012.05.018.

[10] Swift GW. Streaming in thermoacoustic engines and refrigerators. AIP Conf. Proc. 524,105, 2000. doi:10.1063/1.1309184.

[11] Karlsson M, Åbom M, Lalit M, Glav R. A Note on the Applicability of Thermo-Acoustic Engines for Automotive Waste Heat Recovery. SAE Int J Mater Manuf 2016;9:286–93. doi:10.4271/2016-01-0223.

[12] Colonna P, Casati E, Trapp C, Mathijssen T, Larjola J, Turunen-Saaresti T, et al. Organic Rankine Cycle Power Systems: From the Concept to Current Technology, Applications, and an Outlook to the Future. J Eng Gas Turbines Power 2015;137:100801. doi:10.1115/1.4029884.

[13] Horst TA, Tegethoff W, Eilts P, Koehler J. Prediction of dynamic Rankine Cycle waste heat recovery performance and fuel saving potential in passenger car applications considering interactions with vehicles' energy management. Energy Convers Manag 2014. doi:10.1016/j.enconman.2013.10.074.

[14] Freymann R, Strobl W, Obieglo A. The turbosteamer: A system introducing the principle of cogeneration in automotive applications. MTZ Worldw 2008;69:20–7. doi:10.1007/bf03226909.
[15] Bourhis G, Leduc P. Energy and Exergy Balances for Modern Diesel and Gasoline Engines. Oil Gas Sci Technol – Rev l'Institut Français Du Pétrole 2010. doi:10.2516/ogst/2009051.
[16] Bou Nader W, Mansour C, Dumand C, Nemer M. Brayton cycles as waste heat recovery systems on series hybrid electric vehicles. Energy Convers Manag 2018;168:200–14. doi:10.1016/j.enconman.2018.05.004.
[17] Dumont O, Dickes R, Diny M, Lemort V. Experimentation and driving cycle performance of three architectures for waste heat recovery through rankine cycle and organic rankine cycle of a passenger car engine. ECOS 2018 - Proc 31st Int Conf Effic Cost, Optim Simul Environ Impact Energy Syst 2018.
[18] Mansour C, Bou Nader W, Dumand C, Nemer M. Waste heat recovery from engine coolant on mild hybrid vehicle using organic Rankine cycle. Proc Inst Mech Eng Part D J Automob Eng 2019;233:2502–17. doi:10.1177/0954407018797819.
[19] Leduc P, Smague P, Leroux A, Henry G. Low temperature heat recovery in engine coolant for stationary and road transport applications. Energy Procedia 2017;129:834–42. doi:10.1016/j.egypro.2017.09.197.
[20] Smague P, Leduc P, Leroux A. Development of a 48V Orc Turbo-Pump for Waste Heat Recovery in the Coolant of Light Duty and Commercial Vehicles. 5th Int. Semin. ORC Power Syst. Sept. 9 - 11, 2019, Athens, Greece, 2019, p. 1–10.
[21] Hogerwaard J, Dincer I, Zamfirescu C. Analysis and assessment of a new organic Rankine based heat engine system with/without cogeneration. Energy 2013. doi:10.1016/j.energy.2013.09.002.
[22] Oomori H, Ogino S. Waste Heat Recovery of Passenger Car Using a Combination of Rankine Bottoming Cycle and Evaporative Engine Cooling System. SAE Tech. Pap. Ser., 2010. doi:10.4271/930880.
[23] Chang JC, Chang CW, Hung TC, Lin JR, Huang KC. Experimental study and CFD approach for scroll type expander used in low-temperature organic Rankine cycle. Appl Therm Eng 2014;73:1444–52. doi:10.1016/j.applthermaleng.2014.08.050.
[24] Dumont O, Quoilin S, Lemort V. Experimental investigation of a reversible heat pump/organic Rankine cycle unit designed to be coupled with a passive house to get a Net Zero Energy Building. Int J Refrig 2015;54:190–203. doi:10.1016/j.ijrefrig.2015.03.008.
[25] Eborn J, Tummescheit H, Prölß K. AirConditioning – a Modelica Library for Dynamic Simulation of AC Systems. Proc 4th Int Model Conf 2005:185–92. doi:10.1016/j.cep.2011.11.002.
[26] Heidrich P, Krisch T. Assessment of Waste Heat Recovery Options in Passenger Car Applications by Various Rankine Cycles. Heat Transf Eng 2015. doi:10.1080/01457632.2015.995027.
[27] Ciuffo B, Marotta A, Tutuianu M, Anagnostopoulos K, Fontaras G, Pavlovic J, et al. The development of the World-wide Harmonized Test Procedure for Light Duty Vehicles (WLTP) and the pathway for its implementation into the EU legislation. Transp Res Board Annu Meet 2015;15–4935. doi:10.13140/RG.2.1.3175.8562.
[28] Mansour C, Clodic D. Dynamic modeling of the electro-mechanical configuration of the Toyota Hybrid System series/parallel power train. Int J Automot Technol 2012. doi:10.1007/s12239-012-0013-8.
[29] Otter M, Dempsey M, Schlegel C. Powertrain - A Modelica library for modeling and simulation of vehicle powertrains. Model. Work. 2000 Proc., 2000, p. 23–32.
[30] Schweiger C, Dempsey M, Otter M. The PowerTrain Library: New Concepts and New Fields of Application. Proc. 4th Int. Model. Conf., 2005, p. 457–66.
[31] Mansour C, Bou Nader W, Breque F, Haddad M, Nemer M. Assessing additional fuel consumption from cabin thermal comfort and auxiliary needs on the worldwide harmonized light vehicles test cycle. Transp Res Part D Transp Environ 2018;62:139–51. doi:10.1016/j.trd.2018.02.012.
[32] Ferrari G. Motori a combustione interna. Società Editrice Esculapio; 2016.

[33] AP NS. A Simple Engine Cooling System Simulation Model. SAE Tech Pap Ser 2010;1. doi:10.4271/1999-01-0237.
[34] Quoilin S, Desideri A, Wronski J, Bell I, Lemort V. ThermoCycle: A Modelica library for the simulation of thermodynamic systems. Proc 10th Int Model Conf March 10-12, 2014, Lund, Sweden 2014;96:683–92. doi:10.3384/ecp14096683.
[35] Bell IH, Wronski J, Quoilin S, Lemort V. Pure and pseudo-pure fluid thermophysical property evaluation and the open-source thermophysical property library coolprop. Ind Eng Chem Res 2014. doi:10.1021/ie4033999.
[36] Lemort V, Quoilin S, Cuevas C, Lebrun J. Testing and modeling a scroll expander integrated into an Organic Rankine Cycle. Appl Therm Eng 2009;29:3094–102. doi:10.1016/j.applthermaleng.2009.04.013.
[37] Dumont O, Parthoens A, Dickes R, Lemort V. Experimental investigation and optimal performance assessment of four volumetric expanders (scroll, screw, piston and roots) tested in a small-scale organic Rankine cycle system. Energy 2018;165:1119–27. doi:10.1016/j.energy.2018.06.182.
[38] Twomey B, Jacobs PA, Gurgenci H. Dynamic performance estimation of small-scale solar cogeneration with an organic Rankine cycle using a scroll expander. Appl Therm Eng 2013. doi:10.1016/j.applthermaleng.2012.06.054.
[39] Desideri A, Hernandez A, Gusev S, van den Broek M, Lemort V, Quoilin S. Steady-state and dynamic validation of a small-scale waste heat recovery system using the ThermoCycle Modelica library. Energy 2016;115:684–96. doi:10.1016/j.energy.2016.09.004.
[40] Johnson VH. Fuel Used for Vehicle Air Conditioning: A State-by-State Thermal Comfort-Based Approach. SAE Tech Pap Ser 2010;1. doi:10.4271/2002-01-1957.
[41] Fanger PO. Assessment of thermal comfort practice. Occup Environ Med 1973;30:313–24. doi:10.1136/oem.30.4.313.
[42] Benouali J. Etude Et Minimisation Des Consommations Des Systemes De Climatisation Automobile. PhD Thesis at Ecole des Mine de Paris, 2002.
[43] Marcos D, Pino FJ, Bordons C, Guerra JJ. The development and validation of a thermal model for the cabin of a vehicle. Appl Therm Eng 2014;66:646–56. doi:10.1016/j.applthermaleng.2014.02.054.
[44] Crawley DB, Pedersen CO, Lawrie LK, Winkelmann FC. Energy plus: Energy simulation program. ASHRAE J 2000.
[45] Laboe K, Canova M. Powertrain Waste Heat Recovery: A Systems Approach to Maximize Drivetrain Efficiency. ASME 2012 Intern. Combust. Engine Div. Spring Tech. Conf., 2013, p. 985–92. doi:10.1115/ices2012-81160.
[46] von Manstein A, Limperich D, Banakar S. Simulative Comparison of Mobile Air-Conditioning Concepts for Mechanical and Electrical Driven Systems. Proc 12th Int Model Conf Prague, Czech Republic, May 15-17, 2017 2017;132:783–90. doi:10.3384/ecp17132783.
[47] Lemmens S. Cost engineering techniques & their applicability for cost estimation of organic rankine cycle systems. Energies 2016. doi:10.3390/en9070485.
[48] Wang L, Cai W, Zhao H, Lin C, Yan J. Experimentation and cycle performance prediction of hybrid A/C system using automobile exhaust waste heat. Appl Therm Eng 2016;94:314–23. doi:10.1016/j.applthermaleng.2015.10.051.
[49] Salim M. Technical Potential for Thermally Driven Mobile A/C Systems. SAE Tech Pap Ser 2010;1. doi:10.4271/2001-01-0297.